# Uses of Scanning Electrochemical Microscopy in Corrosion Research

**R. M. Souto[1], S. Lamaka[2],** and **S. González[1]**

[1] Department of Physical Chemistry, University of La Laguna, E-38200 La Laguna (Tenerife), Spain
[2] ICEMS, Instituto Superior Técnico, Av. Rovisco Pais, Technical University Lisbon, 1049-001 Lisboa, Portugal

This paper provides a brief review of a relatively new technique, namely scanning electrochemical microscopy (SECM), and its applications in measuring, characterising and evaluating corroding systems. Localized corrosion processes and electrochemical activity distributions in surfaces can thus be investigated in real time with high spatial resolution. The SECM is a unique near-field scanning technique that is electrochemically integrated as to detect chemical and electrochemical activities in electrochemical heterogeneous systems such as those operating in corrosion research. The SECM can be used in a variety of ways, which can be broadly classified into amperometric and potentiometric modes, depending on the type of the sensing probe, namely an ultramicroelectrode (UME) and an ion-selective microelectrode, respectively. The operation modes of the instrument are described together with typical experiments selected to illustrate their application in sensing localised corrosion.

**Keywords** Scanning electrochemical microscopy; corrosion; pitting; delamination; blistering; passivating films.

## 1. Introduction

The function of most metallic components is ultimately limited by corrosion. Metals and alloys spontaneously react with the environment in their tendency to attain other oxidized states which are thermodynamically more stable. Apart from the cost, corrosion consumes huge amounts of materials and the energy required to produce them. Research into corrosion covers mechanisms of corrosion and passivation, methods to control corrosion, either by employing protection procedures such as corrosion inhibition and protective coating layers, and the development of novel processing techniques that would originate materials with improved surface properties.

The degradation reactions occurring at metallic materials exposed to either the atmosphere or to an aqueous environment have in common their electrochemical origin. This is the reason that a major part of the current knowledge of corrosion processes has been gained from the use of conventional electrochemical methods in the corrosion laboratory, though these techniques lack spatial resolution and provide little information on behaviour at sites of corrosion initiation or at defects. Indeed, corrosion reactions have traditionally been considered to initiate within the range of nanometers and micrometers, though there were not available techniques for the investigation of these processes in those scales. Furthermore, electrochemical heterogeneity is also a typical characteristic of most metallic materials, particularly applicable in the case of alloys and joined metals, but also in the case of single metal materials. The problem of surface inhomogeneity is even more acute as corrosion protection methods usually involve chemical modification of surfaces. Thus, there is need for ancillary techniques with enhanced spatial resolution which can acquire data in real time, and can provide corroborative or other novel evidence of the underlying reaction schemes preferably *in situ*.

New methods of probing the microscopic processes on electrode surfaces have recently been developed in the field of Electrochemistry. Among them, scanning microelectrochemical techniques, which are an extension of local probe techniques originating from the use of microelectrodes as the probes in near field microscopic techniques to operate inside an electrochemical cell, are concentrating major interest. In this way, the chemical and/or electrochemical selectivities provided by the microelectrode probes can be successfully combined with the spatial resolution of the scanning microscopies, thus allowing surface characterization with a resolution in the micrometer range or below. Among these techniques, scanning electrochemical microscopy (SECM) was designed in 1989 by Bard and coworkers [1], and since then, the SECM has become a very powerful technique for probing a great variety of electrochemical processes in fundamental and applied electrochemistry [2], energy storage [3], materials science [4], corrosion science [3,5], biosensors research [6] and biophysics [7].

In this contribution, the operation modes of SECM will be described and selected applications in the investigation of corrosion reactions will be provided in order to illustrate its application in sensing localised corrosion.

## 2. Principles of SECM operation

The SECM instrument basically consists of a combination of electrochemical components, positioners and computer control. Figure 1 shows a schematic diagram of the basic SECM instrument employing an amperometric microprobe. The SECM is a technique in which a current flows through a microelectrode immersed in an electrolytic solution and situated close to a substrate. The substrate can either be a conductive, semiconductive or insulating material. The

microelectrode and the substrate form part of an electrochemical cell which is also constituted by reference and auxiliary electrodes, and sometimes by a second working electrode. The electrochemical setup is constituted by this electrochemical cell together with the bipotentiostat, which is the actual electrochemical interface. It allows the potential of the microelectrode and/or the substrate versus the reference electrode to be controlled, as well as to measure the current flowing between any of the working electrodes and the counter electrode. The microelectrode displacement and its position relative to the substrate are controlled with a three-dimensional microstage that provides independent and accurate control in the *x*-*y*-*z* axis. And the remaining component is the data acquisition and display system, usually conformed by a computer, an interface and a display system.

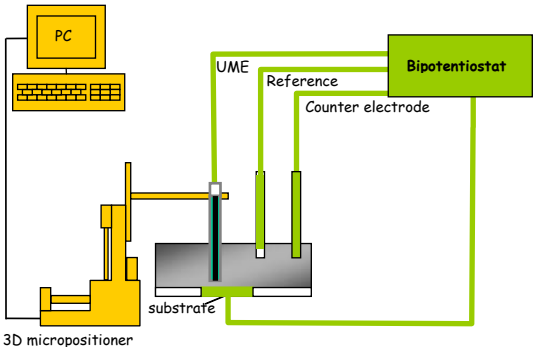


**Fig. 1** Diagram showing the main components of the SECM instrument.

The microelectrode is a microdisc electrode, in which the electrode material is surrounded by an insulating shield. The most common procedure for its fabrication is the encapsulation of the electrode material (carbon fibres or metal wires) in glass capillaries and the subsequent polishing of the tips to expose the microdisc surface. At this point, it is possible to distinguish two kinds of microelectrodes depending on the ratio between the insulating-shield thickness (*b*) to the disc-electrode radius (*a*) (see Figure2), $RG = b/a$, namely,

- Microelectrodes with infinite insulating shield ($RG>10$), and
- Microelectrodes with finite insulating shield ($RG<10$), in which the insulating-shield thickness is comparable to the electrode radius.

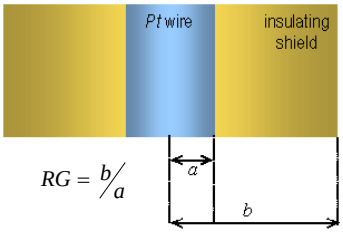


**Fig. 2** Schematic view of a disc microelectrode tip and the parameters that define the *RG* value.

The latter types of microelectrodes are those generally used as tips in SECM measurements. It must be considered that, for microelectrodes with $RG<10$, on the time scale of standard voltammetric measurements, the diffusion field undergoes a transition from linear to radial symmetry, and it is established behind the plane of the disc-electrode and the insulating shield as is shown in Figure 3.

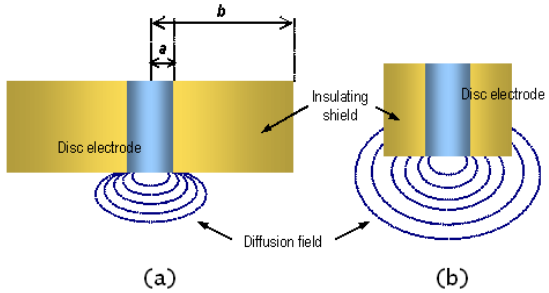


**Fig. 3** Scheme of the geometry and diffusion field for a disc microelectrode having (a) $RG \geq 10$, and (b) $RG \leq 2$.

Prior to explaining the operation and the response of the SECM, it is necessary to understand the behaviour of the microelectrode inside an electrochemical cell. Let's consider the microelectrode is immersed in a solution containing an electrolyte and a reducible species, *O*. When a potential sufficiently negative to the standard potential of the reduction

reaction (1), is applied to the microelectrode, the reduction of the species *O* occurs at the UME surface, and a cathodic current flows according to:

$$O + ne^- \leftrightarrow R \qquad (1)$$

If this reaction is kinetically controlled by the diffusion of *O* from the bulk of the solution to the electrode surface, the current decays due to the formation of a diffusion layer of *O* around the electrode, and attains rapidly a steady-state value given by

$$i_{T,\infty} = 4nFDca \qquad (2)$$

where *F*, is the Faraday constant; *a*, the microelectrode radius; *D*, the diffusion coefficient of the reducible species; and, *c*, its concentration. That is, a steady-state current (see Figure 4) results from the constant flux of *O* to the electrode surface due to an expanding hemispherical diffusion layer around the microelectrode.

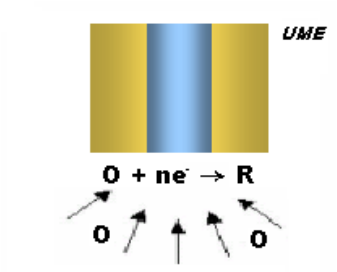


**Fig. 4** Schematics of the SECM setup in the amperometric mode when the UME is placed in the bulk of the electrolytic solution, without any interference from the substrate. Reducible species *O* is considered to be electroreduced to species *R* at the SECM-UME.

The current measured at the microelectrode depends on the relative size of the disc electrode and shield. Therefore, the equation predicting the steady-state limiting current for a disc-microelectrode equation (2) is not valid for microelectrodes with low *RG*, and corrections to the theoretical expression must be introduced.

The standard procedure employed for the characterization of a given microelectrode involves two experimental steps, namely to record a cyclic voltammogram in the bulk of electrolyte and to measure an approach curve towards a substrate, in solutions containing a well-known redox system (cf. Figure 5).

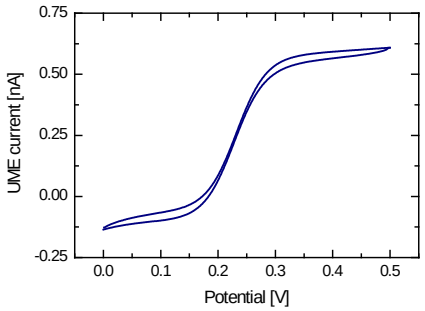


**Fig. 5** Cyclic voltammogram measured at the SECM-tip in 0.5 mM ferrocene-methanol + 0.1 M KCl. Scan rate: $v$ = 0.01 V $s^{-1}$. It depicts the electrochemical reactions associated with dissolved ferrocene in the electrolyte.

An estimation of the radius of the microelectrode can be made from the steady-state limiting current obtained in the voltammetry at low scan rates and using the steady-state equation (2), because it relates limiting current on the microelectrode with the concentration of the redox species and the electrode radius. This expression is only valid for microelectrodes with $RG > 10$. In the case of disc-electrode with $RG < 10$, in which $b$ is known, the radius can be estimated using the equation (3), which relates the $RG$ parameter ($b/a$) with characteristic parameters from the voltammograms [8]:

$$\frac{b}{a} = RG = A_o + A_1\left(\frac{b-a}{\delta}\right) + A_2\left(\frac{b-a}{\delta}\right)^2 + A_3\left(\frac{b-a}{\delta}\right)^3 \qquad (3)$$

In the equation (3), $A_i$ are coefficients which depend on the difference between $E_{1/2}$ values for the reduction and oxidation waves in the cyclic voltammogram ($\Delta E_{1/2}$) and $\delta$ is the length which is related to the scan rate in the way $\left[RTD/nFv\right]^{1/2}$ where $v$ is the scan rate.

On the other hand, the estimation of the ratio between the insulating shield and the microelectrode radius (*RG* parameter), can be made from the fit of experimental and theoretical approach curves. In brief, the approach curve is obtained by slowly approaching the surface with the tip and simultaneously recording the measured current at the microelectrode *vs. Z* displacement as described elsewhere [9]. This procedure consists on fitting the experimental approach curves measured at the microelectrode, by using a redox mediator in the solution, to theoretical approach curves calculated for various *RG* values. Theoretical approach curves at microdiscs for either negative or positive feedback are described by equations (4) and (5), respectively, which were derived using digital simulation procedures [10].

$$I(L) = \frac{1}{K_1^N + K_2^N / L + K_3^N \exp\left(K_4^N / L\right)} \tag{4}$$

$$I(L) = K_1^P + \frac{K_2^P}{L} + K_3^P \exp\left(-K_4^P / L\right) \tag{5}$$

In these equations, *I(L)* is the normalised steady-state tip current, and *L* is the normalised tip-substrate distance. The parameters $K_i^N$ and $K_i^P$ are numerical constants that depend on the *RG* parameter and the type of feedback, and their values have been evaluated by several authors [11,12]. Two approach curves measured at SECM-tips in a ferrocene-methanol containing solution whereas approaching a polyurethane-coated carbon steel sample exposed to the solution are depicted in Figure 6.

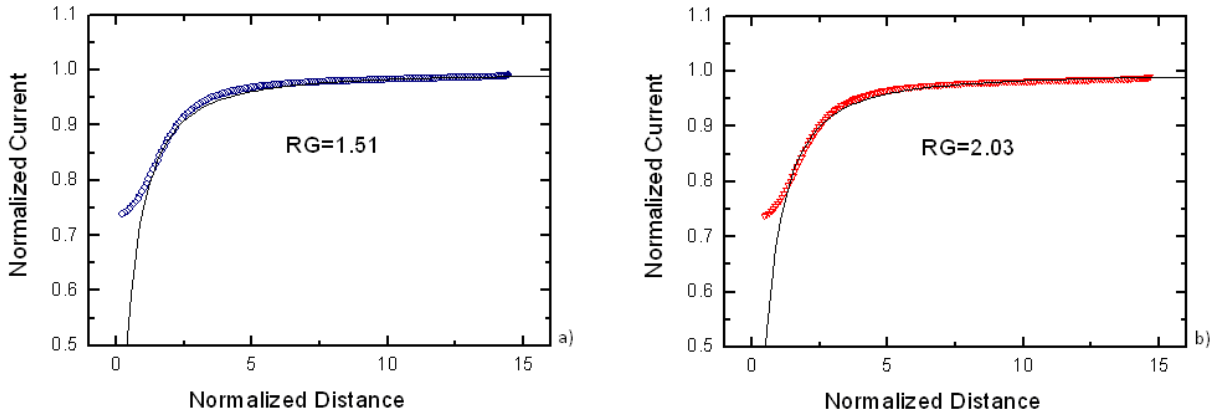


**Fig. 6** Approach curves measured at SECM-tips in 0.1 M KCl + 0.5 mM ferrocene-methanol solution shortly after the polyurethane-coated carbon steel samples were exposed to the solution. Tip potential: +0.50 V *vs.* Ag/AgCl/KCl (saturated) reference electrode.

## 3. Operation modes of the SECM

There are several modes of operation of the scanning electrochemical microscope that have successfully been employed to the characterization of corrosion processes. They are namely,

3.1 Negative feedback mode: Monitoring of blister corrosion in polymer-coated metals [13-18].

In general, feedback modes require an oxidizable/reducible species to be added in the solution phase for SECM operation. This species is known as the redox mediator. Generally redox couples involving a fast, usually one-electron, heterogeneous reaction at the tip are chosen as electrochemical mediators. The faradaic current related to the redox transformation of the mediator is thus measured at the tip, usually by setting the tip potential at a value sufficiently far from its corresponding standard potential to achieve a diffusion-limited regime. In this mode, the SECM tip is rastered in the *X-Y* plane of the surface of the sample inside an electrochemical cell. In SECM, the proximity of the tip to the substrate is the perturbation in the measurement that constitutes the SECM response [1].

If the UME is brought to the vicinity of an insulating substrate, the steady-state current that flows through the tip, $i_T$, tends to be smaller than $i_{T,\infty}$ (Figure 7). This is a result of the insulating substrate partially blocking the diffusion of *O* towards the tip [19]. The current at the tip becomes smaller when the tip is closer to the substrate, and tends to zero when the distance between tip and substrate, *d*, approaches zero. This effect is known as negative feedback.

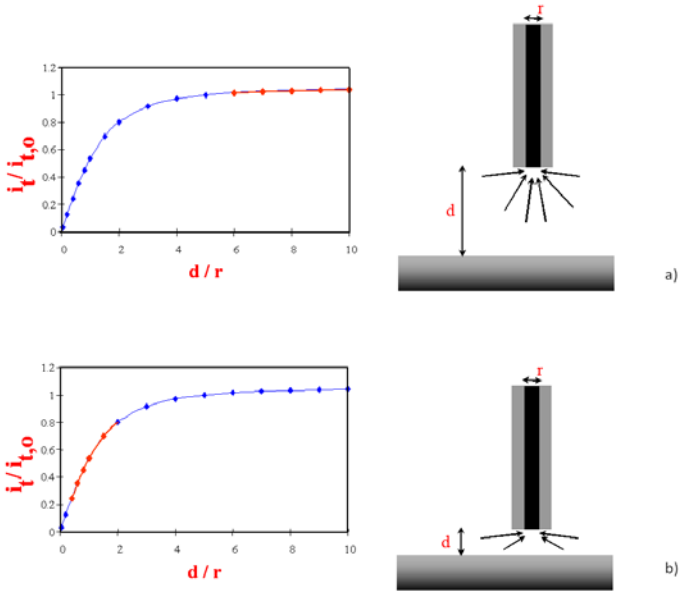


**Fig. 7** The negative-feedback mode of SECM and its effect on the approach curve measured when the tip is moved towards an insulating substrate: a) the tip is located far from the surface where the hemispherical diffusion regime of the mediator is maintained; and b) the tip is located in close proximity to the substrate; the faradaic current measured at the tip is significantly smaller than $i_{T,\infty}$ due to the hindered diffusion of the mediator. The portion of the curves drawn in red on the approach curves indicate the range of currents related to the corresponding scheme at the right side of the figure.

As it can be observed from the inspection of Figure 7, the feedback effect is sensitive to the distance between the tip and the substrate, *d*, which is often expressed in units of the tip radius, *a*, as $L=d/a$. Surface imaging of insulating substrates can be thus directly accomplished when the tip is rastered over the sample in the *constant height* mode. In this way, the tip is lowered to a fixed distance from the substrate and then the surface is scanned. Changes in the faradaic current measured at the tip are then exclusively related to variations in the distance between the tip and the substrate underneath, which originate from the scanned surface either progressing in the solution towards the tip (resulting in smaller faradaic currents being measured at the tip), or the surface showing a depression (higher faradaic currents are measured in this case). The currents measured at the tip can be rapidly converted to a height or distance scale. The resolution of the SECM in topographic measurements on a surface strongly depends on the tip radius, *a*.

Operation of the SECM in the negative feedback has allowed for specific anion effects towards early blistering stages at polymer coated metals to be detected for the first time. Chloride ions have been thus shown to produce significant roughening of the polymer surface related to heterogeneous electrolyte distributions at the metal-polymer interface in a wide variety of systems [13-16], as well as to monitor the growth of individual blisters by using the approach curves to correlate current values to tip-substrate distances [17,18]. It must be noticed that a common procedure in those studies consists in using an inverted *Z*-axis for SECM mapping, in order that protrusions and hills existing on the surface can be viewed as higher areas in the map though they are really detected from the measurement of smaller faradaic currents at the tip. Figure 8 depicts both a scheme of the process and the SECM images obtained after a PVC-coated galvanized steel was immersed in 0.5 M NaCl aqueous solution containing ferrocene-methanol as electrochemical redox mediator (see Figure 8).

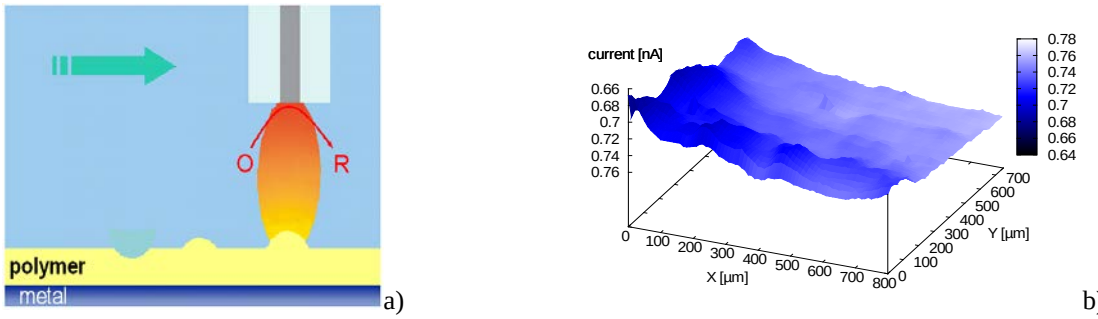


**Fig. 8** Surface imaging of insulating substrates with the SECM operating in the negative-feedback mode. a) Scheme describing hills and depressions in the surface of the polymeric film deposited on the metal and their effect on the current measured at the tip; b) Image generated by SECM of a PVC-coated sample immersed in 0.5 M NaCl + 5 mM ferrocene-methanol. The image was taken after 6 hours immersion, and represents 800 µm x 700 µm in *X* and *Y* directions. The *Z* scale is the tip current in nA. Tip potential, +0.50 V versus the Ag/AgCl/KCl (saturated) reference electrode.

3.2 Positive feedback mode: Characterization of passivating film formation by corrosion inhibitors on copper [20-23].

Conversely to what happens in the previous mode, if the tip is close to a conductive substrate at which the oxidation reaction (6) can occur, a flux of *O* from the substrate to the tip occurs, in addition to some flux from the bulk solution towards the tip.

$$R \leftrightarrow O + ne^- \qquad (6)$$

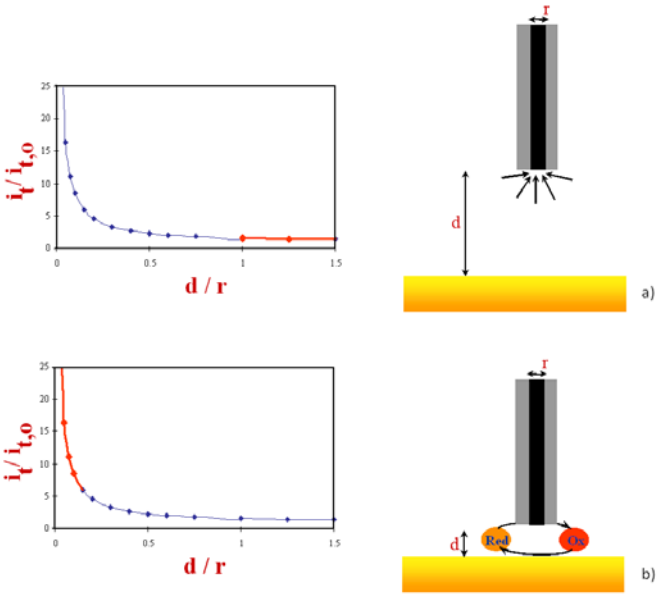


**Fig. 9** The positive-feedback mode of SECM and its effect on the approach curve measured when the tip is moved towards a conducting substrate: a) the tip is located far from the surface where the hemispherical diffusion regime of the mediator is maintained; and b) the tip is located in close proximity to the substrate; the faradaic current measured at the tip is significantly greater than $i_{T,\infty}$ due to the regeneration of the mediator. The portion of the curves drawn in red on the approach curves indicate the range of currents related to the corresponding scheme at the right side of the figure.

This effect leads to an enhancement of the current at the tip, $i_T$, which is higher than $i_{T,\infty}$ (Figure 9). Then the flux of *O* from the substrate to the tip causes an increase of $i_T$ as *d* decreases. In this case, when the tip-substrate distance approaches zero, the $i_T$ current tends to infinite, and the oxidation of *R* on the substrate is diffusion-controlled. This effect is named positive feedback. The tip can be seen as both the generator of the signal sensing the substrate (the flux of the reduced species, *R*), and the detector (of the flux of *O* from the substrate).

The SECM can be used as an electrochemical tool to study electrode processes and coupled homogeneous reactions. In this mode the *XY*-plane scanning is often not used. Commonly, the SECM electrochemical measurements combine the features of the microelectrodes and the advantages of thin-layer electrochemistry [24]. This mode is useful in the determination of heterogeneous electron-transfer reaction rates. The magnitude of the feedback effect is determined by the rate of mediator regeneration at the substrate, thus allowing for information on the kinetics of the process at the substrate to be acquired from the measured approach curves. This is the rational of SECM for the investigation of thin inhibitor films formed on reactive metals, in order to investigate the kinetics of film formation [20,23], as well as to ascertain the effect of chemical and electrical parameters on this process [21,22]. Figure 10 shows changes in the shape of approach curves towards a copper surface exposed to an aqueous solution containing benzotriazole, which is a widely recognized inhibitor for copper corrosion. The measurements were used in a solution containing ferrocene-methanol as electrochemical mediator and $Na_2SO_4$ as base electrolyte. The magnitude of the positive feedback effect is observed to decrease with the elapse of time, a clear indication that the rate of mediator regeneration at the substrate decreases accordingly. Thus, the conductive character of the copper surface towards electron transfer at the metal/electrolyte interface is progressively shadowed with the progress of the chemical interaction between the inhibiting organic molecule and the metal [23].

From the foregoing it can be seen that SECM allows to make quantitative electrochemical measurements in very small domains (consider the tiny gap volume between tip and sample) with small amounts of material. Nevertheless some special care must be taken as to secure that the electrical state of the substrate is adequately controlled. Though operation in open circuit conditions, namely the spontaneous corrosion potential of the system, is desired, the addition to the test electrolyte of an electrochemical redox mediator for visualization purposes at the SECM effectively acts as externally polarizing the substrate, though a potential value would not be applied to the substrate with the potentiostat [2]. This is because the Nernst equation for the redox mediator applies, and the potential of the substrate will be

controlled by the ratio $(c_O/c_R)$. Therefore, the choice of redox mediator must be made with care on the basis of the corresponding $E^0_{O/R}$ values to avoid the undesired polarization of the substrate [23]. Additional care must be taken to discard a simultaneous interaction between the active species in the electrolytic phase (i.e. the corrosion inhibitor organic compound) and the microelectrode tip, otherwise the electrochemical condition of the tip will be continuously varying during the experiment, and the variations in the faradaic current measured at the tip will not exclusive result from changes in the activity of the investigated substrate [23].

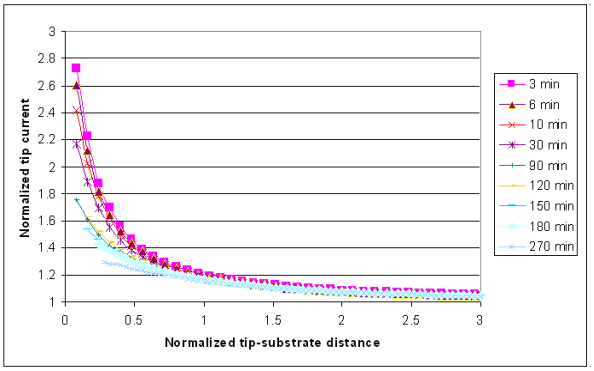


**Fig. 10** Normalized approach curves towards a copper surface measured in a 0.067 M $Na_2SO_4$ + 0.33 mM BTAH + 0.67 mM ferrocene-methanol solution with a 25 μm Pt electrode. Tip potential: +0.50 V vs. Ag/AgCl, KCl (3M). The curves were measured for the immersion times indicated in the figure.

### 3.3 Sample generation – tip collection mode: Detection of metastable pitting in stainless steel [25].

In generation-collection modes, a faradaic current is measured at the tip arising either from a species generated at the surface of the material under imaging (sample generation – tip collection mode), or from a species generated at the tip (tip generation – sample collection mode). A faradaic current is measured at the tip. The ratio between the fluxes at the tip and at the substrate define the collection efficiency, and it is strongly affected both by the relative size of tip and substrate, and by the tip-substrate distance. Furthermore, in these SECM modes, the substrate can be either polarized or left unbiased.

In the sample generation – tip collection mode (SG/TC), the current at the microelectrode arises from a species generated at the surface of the imaged material as depicted in Figure 11a, and the tip moves inside a thick diffusion layer generated by the substrate.

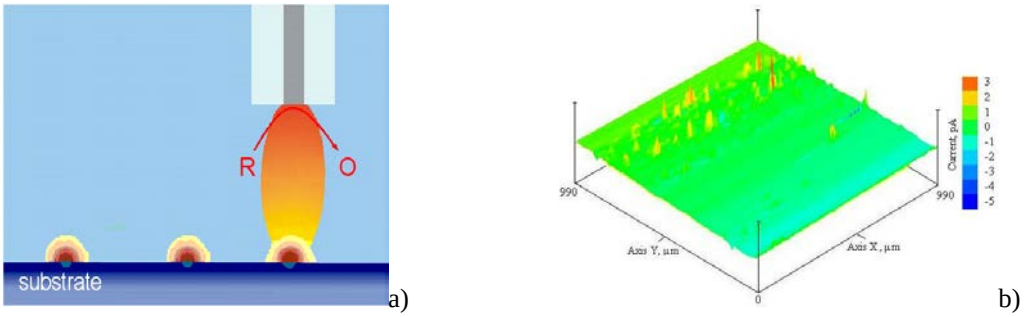


**Fig. 11** Surface imaging of a spontaneously-corroding substrate with the SECM operating in the sample generation – tip collection mode. a) Scheme describing local sources of metal ions in the surface and their effect on the current measured at the tip as they are further electrooxidized; b) SECM image of 304 stainless steel surface immersed in 0.5 M HCl solution at the open-circuit corrosion potential. The image shown represent an area of 1000 μm x 1000 μm in *X* and *Y* directions. Tip potential: +0.50 V *vs.* Ag/AgCl/KCl (saturated) reference electrode. Tip-substrate distance: 10 μm. The background current was taken as zero.

In the amperometric mode, the reaction at the tip may affect the diffusion layer at the substrate. Therefore, special care must be taken in order to adequately select the scan parameters to minimize convective effects, because the tip agitates the diffusion layer at the substrate [26]. Though collection efficiency is low, making quantitative analysis difficult [27,28], this operation mode finds extensive application in the study of localized corrosion processes [25-30] due to the combined effect of selective detection of reacting species liberated in the reactions and the operation of the corroding cell in spontaneous conditions without the need to introduce electrochemical mediators for imaging.

Collection efficiency can be enhanced by employing chemically modified tips, namely with deposits of mercury or bismuth, because they allow to accumulate the redox species liberated during the scan and subsequently analyze it by stripping voltammetry [31]. This application is illustrated in Figure 12, corresponding to the SECM study of a Fe-Zn galvanic couple spontaneously corroding in a chloride-containing solution by using a mercury sphere-cap microelectrode tip [32,33].

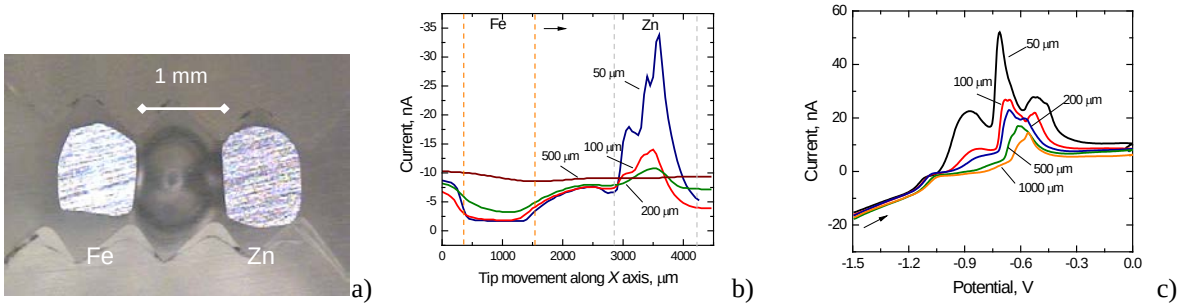


**Fig. 12** Visualization of corrosion reactions occurring for an iron-zinc couple immersed in 0.1 M NaCl. a) Optical image of the sample. b) Line scans of a sphere-cap microelectrode travelling over the Fe-Zn pair; tip potential: –1.2 V *vs.* Ag/AgCl/KCl (saturated) reference electrode. c) Stripping voltammograms of the Zn-deposited in the Hg-electrode during the measurements of line scans given in Figure 12b. The plots corresponded to different tip-sample distances as indicated. Potential values are given *vs.* Ag/AgCl/KCl (saturated) reference electrode. Sphere-cap parameters: $H = 1$, $RG = 5$.

This method has allowed the metastable pitting of a passivated metal substrate to be imaged for the first time [25]. The state is interesting because it is a precursor state to stable pitting and appears to be controlled by the same mechanism as that of stable pitting [34]. A SECM image describing metastable pits on 304 stainless steel obtained in situ in chloride solution at the open-circuit corrosion potential is shown in Figure 11b. This image represents the oxidation of $Fe^{2+}$ emanating from the metastable pits as the probe tip passed over them. It can be easily deduced that the lifetime of the detected pits was a maximum of a few seconds since they are not observed on the following scanline.

### 3.4 Tip generation – sample collection mode: Generation of corrosion pits on iron [35-37].

This operation mode is base on the generation of a chemical species at the tip that will be sensed at the substrate (see Figure 13a), either to be detected through its faradaic conversion to a different oxidation state, or to locally modify the chemistry of the substrate. Conversely to what happens in the SG/TC mode, due to the relative sizes of the substrate and the tip, the collection efficiency in mode TG/SC is close to 100% for a stable species, whereas collection efficiencies differing from 100% can be employed to investigate homogeneous chemical kinetics.

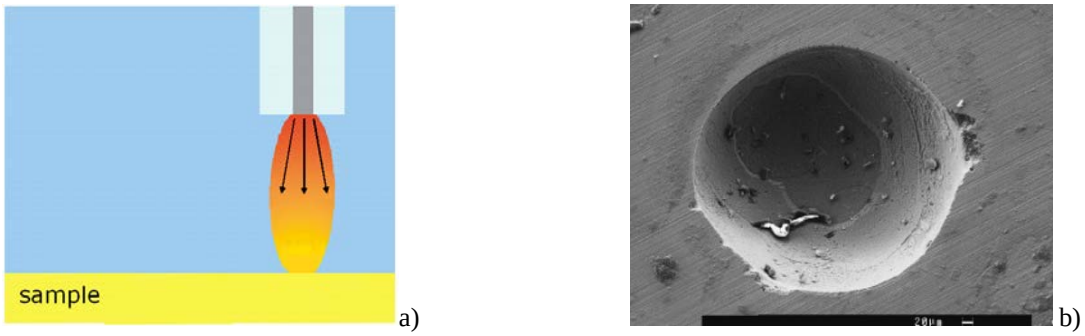


**Fig. 13** The tip generation – sample collection mode of SECM: a) scheme of the operation procedure; and b) SEM observation of a single pit generated on iron by SECM technique in 0.5 M $H_2SO_4$ solution. Reprinted from [37]. Copyright 2008, Elsevier Science Ltd.

The high collection efficiency of the method has been employed to the localized generation of corrosion pits. As pitting is a random phenomenon, it is very difficult to predict the position and the time for its occurrence. Therefore, SECM can alternately be employed to induce the generation of a single pit at passivated surfaces. This is possible due to the fast generation of a locally aggressive environment at a preselected site of the substrate. The kinetics of pit growth can be then investigated from the measurement of the faradaic current flowing at the substrate [35]. Additionally, SECM could also be employed in combination with the electrochemical quartz microbalance, allowing for higher sensitivities to be attained [36,37]. A SEM image of a single pit formed on pure iron as result of the release of free chloride ions at the SECM tip is shown in Figure 13b.

3.5 Redox competition mode: Visualization of delamination reactions from defects exposing the underlying metal in painted systems [38,39].

When the soluble redox species monitored at the tip can also undergo redox transformation on the substrate, a new operation mode for SECM is encountered, which is called redox competition. That species can either be naturally occurring in the environment [38], or be *in situ* generated by employing an electrochemical programme based on the application of a series of potentiostatic pulses [40,41]. Whereas the later procedure allows for a controlled concentration of the species to be generated locally, the former presents the advantage that natural conditions, such as those operating in corrosion processes, can be used without further chemical modification of the system.

Usually, dissolved oxygen in the electrolyte is the redox species employed in the redox competition mode. Since this is an electroactive molecule, the need for the addition of a redox mediator is alleviated for SECM operation. Furthermore, in the case of freely corroding systems, soluble oxygen directly participates in the corrosion processes through electroreduction at the cathodic sites. Therefore, the tip and the sample under investigation compete for the same redox species in solution [42], and the scanning electrochemical microscope is to be operated in the redox competition mode as depicted in Figure 14a.

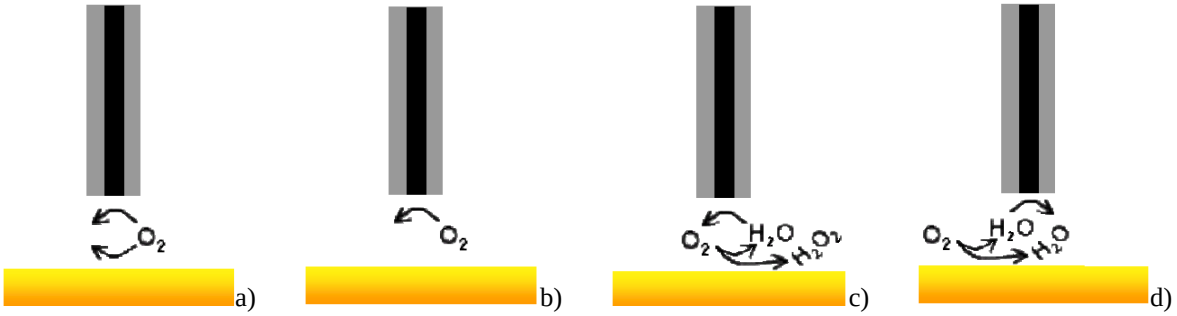


**Fig. 14** Schemes of the various SECM operation modes that can operate on the redox transformation of soluble oxygen in the electrolytic phase, namely: a) redox competition, b) TG/SC, c) SG/TC, and d) negative feedback modes.

The use of oxygen as redox mediator for SECM allows to image both the topography and the interfacial processes in defective organic coatings applied on metallic substrates [38,39]. The maps provided only topographical information when the uncoated metal is stable in the environment, whereas the maps were a combination of the topography and the electrochemical reactivity of the sample in the case the metal freely corrodes from the defects [39]. This is the case when a carbon steel substrate coated with an epoxy-polyamine film, in which a circular defect has been produced with a drill, was immersed in a sulphate-containing solution as illustrated in Figure 15.

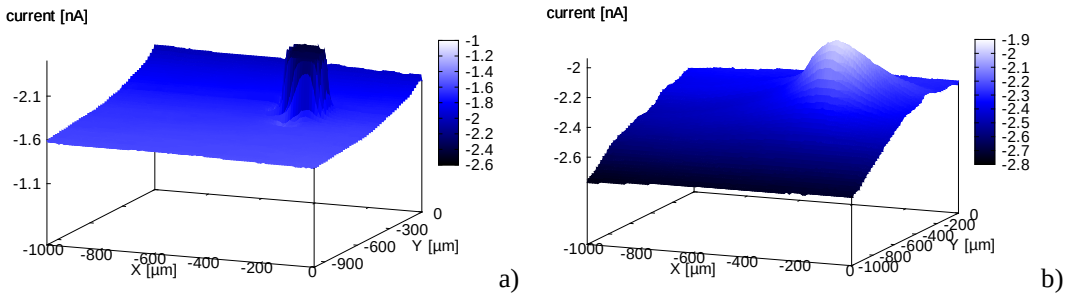


**Fig. 15** SECM images of an epoxy-polyamine coated carbon steel sample after immersion in 0.1 M $Na_2SO_4$ air-saturated aqueous solution for: a) 5, and b) 450 min. Tip-substrate distance: 15 µm. Tip potential: -0.60 V *vs.* Ag/AgCl/KCl (saturated) reference electrode. The figures represent an area of 1000 µm x 1000 µm in *X* and *Y* directions. It must be noticed that the current axis are allocated in the opposite directions in the two figures.

Redox transformation of soluble oxygen at the SECM can originate various operation modes, namely:

- Redox competition. The tip detects the reduction current for $O_2$. The measured current decreases locally due to the local depletion in oxygen concentration due to oxygen consumption at the tip (Figure 14a).
- Negative feedback. The tip detects the reduction current for $O_2$. Diffusion of the redox species is hindered by the insulating substrate (Figure 14b).
- Tip-generation and sample-collection (TG/SC mode). The tip is employed to oxidize water resulting in the production of $O_2$. The signal measured arises from $O_2$ reduction at the substrate (Figure 14c).

- Sample-generation and tip-collection (SG/TC mode). The substrate is polarized to reduce $O_2$. The tip oxidizes $H_2O_2$ generated as by-product on the substrate. The analytical signal is the oxidation current for peroxide detected at the tip (Figure 14d).

### 3.6 Potentiometric mode: Measurement of local pH variations and concentrations of dissolving metal ions during galvanic corrosion.

In potentiometric mode a potential difference between the ion-selective tip and a reference electrode is measured under zero current conditions. Thus, the tip is a passive sensor which neither generates nor collects any ionic species. The ion-selective tip does not influence significantly local corrosion events; it detects variations of specific ion activity in the vicinity of the corrosion sites. The ion-selective tip has to be calibrated before and after measuring ion activity. In general, the potential of the ion-selective tip, $E_i$, depends on activity of a specific ion in solution, $a_i$, as provided by the well known Nernst equation: $E_i = const + \frac{RT}{z_i F} \ln a_i$ [10,43,44].

The diversity of corrosion processes, to a great extent, results from the complexity of acid-base reactions accompanying redox conversions. Naturally, analysis of acid-base interactions during the course of corrosion processes is the most common type of localized potentiometric measurements [43,45]. Figure 16 presents an example of pH mapping taken with a pH-selective glass-capillary microelectrode over coupled Al and Cu wires. The tip diameter was 2 µm and the liquid membrane based on 4-nonadecylpyridine (95295 Fluka) as ionophore. Anodic dissolution of aluminium accompanied by hydrolysis of hydrated $Al^{3+}$ cations leads to local acidification over the Al wire while cathodic reduction of oxygen taking place on Cu results in local alkalinisation.

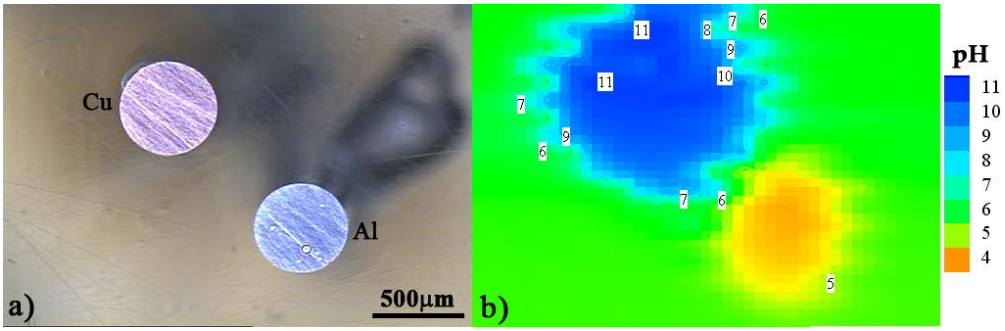


**Fig. 16** An example of pH measurements over the coupled Cu and Al wires: Optical micrograph of Cu and Al wires embedded into epoxy holder (a) and corresponding pH distribution recorded in 0.05M NaCl solution (b).

Modelling of corrosion processes and corrosion prediction requires an extensive database of input data, including time-dependant distribution of pH and dissolving metal cations ($Mg^{2+}$, $Al^{3+}$, $Zn^{2+}$, $Fe^{3+}$ etc.). The ions of supporting electrolyte, e.g. $Cl^-$ and $Na^+$, participate in charge compensation processes [46], hence the knowledge on their distribution is also very important. Activity of a specific ion can be measured by using tips selective to that specific ion. Figure 18 shows the map distribution of $Mg^{2+}$ cations over a dissolving Mg wire. The data was recorded using a glass-capillary tip with the liquid membrane selective to $Mg^{2+}$ (N,N″-octamethylene-bis(N′-heptyl-N′-methyl-methylmalonamide), Fluka 63083 [47].

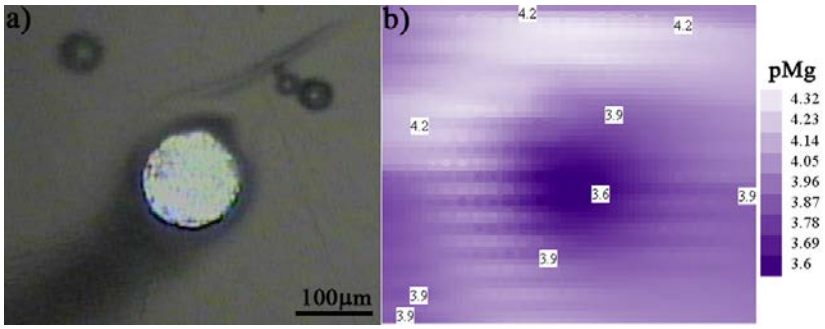


**Fig. 17** Optical micrograph of a 0.125 mm diameter, pure Mg wire in epoxy holder (a) and corresponding distribution of $Mg^{2+}$ ions ($pMg = -\log_{10}[Mg^{2+}]$) recorded in 0.05M NaCl solution (b).

The main advantage of ion-sensitive glass-capillary tips with liquid membrane is that the same procedure is used to prepare the tips selective to different ions. Only the composition of the liquid membrane has to be changed in order to produce a tip selective to another ion. A drawback of tips of this type is that they lack tip-to-substrate distance sensitivity. To follow the topography of a substrate a double-barrel glass-capillary microelectrode can be used [44]. One channel of the Θ shape micropipette, filled with an electrolyte solution, is used as a distance sensor while the second channel, with the tip filled with the liquid membrane, is ion-sensitive. Another approach to perform constant-distance SECM measurements with glass-capillary tip is to use non-optical shear force detection by attaching two piezoelectric plates to the tip [48,49].

## 4. Concluding remarks

SECM is a powerful technique for studying corrosion processes because it allows for *in situ* characterization of both topography and localized corrosion activity in micrometer and submicrometer ranges. The wide variety of operation modes, with or without redox mediators, allows to gather analytical information and quantify local corrosion processes in real time for a variety of localized corrosion reactions, with multiple applications including microscopic defects at the metal/passive film/electrolyte interface, coatings, adsorption of inhibitor films, metal electrodissolution, and others.

**Acknowledgements** The support by Ministerio de Ciencia y Tecnología (Spain) and Fundação para a Ciência e a Tecnología (Portugal) under Projects No. CTQ2009-12459, CTQ2009-14322 and PTDC/CTM/108446/2008 is gratefully acknowledged.

## References

[1] Bard AJ, Fan F-RF, Kwak J, Lev O. Scanning electrochemical microscopy. Introduction and principles. *Analytical Chemistry.* 1989;61:132-138.
[2] Mirkin MV, Horrocks BR. Electroanalytical measurements using the scanning electrochemical microscope. *Analytica Chimica Acta.* 2000;406:119-146.
[3] Pust SE, Maier W, Wittstock G. Investigation of localized catalytic and electrocatalytic processes and corrosion reactions with scanning electrochemical microscopy (SECM). *Zeitschrift für Physikalische Chemie*. 2008;222:1463-1517.
[4] Sun P, Laforge FO, Mirkin MV. Scanning electrochemical microscopy in the 21st century. *Physical Chemistry Chemical Physics*. 2007;9:802-823.
[5] Niu L, Yin Y, Guo W, Lu M, Qin R, Chen S. Application of scanning electrochemical microscope in the study of corrosion of metals. *Journal of Materials Science*. 2009;44:4511-4521.
[6] Stoica L, Neugebauer S, Schuhmann W. Scanning electrochemical microscopy (SECM) as a tool in biosensor research. *Advances in Biochemical Engineering and Biotechnology*. 2008;109:455-492.
[7] Edwards MA, Martin S, Whitworth AL, Macpherson JV, Unwin PR. Scanning electrochemical microscopy: principles and applications to biophysical systems. *Physiological Measurement*. 2006;27:R63-R108.
[8] Ciani I, Daniele S. Voltammetric determination of the geometrical parameters of inlaid microdisks with shields of thickness comparable to the electrode radius. *Analytical Chemistry.* 2004;76:6575-6581.
[9] Souto RM, González-García Y, González S. Evaluation of the corrosion performance of coil-coated steel sheet as studied by scanning electrochemical microscopy. *Corrosion Science.* 2008;50:1637-1643.
[10] Bard AJ, Mirkin MV, eds. *Scanning Electrochemical Microscopy.* New York: Marcel Dekker; 2001.
[11] Amphlett JL, Denuault G. Scanning electrochemical microscopy (SECM): An investigation of the effects of tip geometry on amperometric tip response. *Journal of Physical Chemistry B.* 1998;102:9946-9951.
[12] Harriman K, Gavaghan DJ, Houston P, Suli E. Adaptive finite element simulation of currents at microelectrodes to a guaranteed accuracy. Theory. *Electrochemistry Communications.* 2000;2:157 -162.
[13] Souto RM, González-García Y, González S, Burstein GT. Damage to paint coatings caused by electrolyte immersion as observed *in situ* by scanning electrochemical microscopy. *Corrosion Science.* 2004;46:2621-2628.
[14] Souto RM, González-García Y, González S. Evaluation of the corrosion performance of coil-coated steel sheet as studied by scanning electrochemical microscopy. *Corrosion Science.* 2008;50:1637-1643.
[15] Souto RM, González-García Y, González S. Characterization of coating systems by scanning electrochemical microscopy: surface topology and blistering. *Progress in Organic Coatings.* 2009;65:435–439.
[16] Souto RM, González-García Y, Izquierdo J, González S. Examination of organic coatings on metallic substrates by scanning electrochemical microscopy in feedback mode: revealing the early stages of coating breakdown in corrosive environments. *Corrosion Science.* 2010;52:748-753.
[17] Souto RM, González-García Y, González S, G.T. Burstein GT. Imaging the origins of coating degradation and blistering caused by electrolyte immersion assisted by SECM. *Electroanalysis.* 2009;21:2569-2574.
[18] González-García Y, Santana JJ, González-Guzmán J, Izquierdo J, González S, Souto RM. Scanning electrochemical microscopy for the investigation of localized degradation processes in coated metals. *Progress in Organic Coatings.* 2010; doi:10.1016/j.porgcoat.2010.04.006.
[19] Bard AJ, Denuault G, Lee C, Mandler D, Wipf DO. Scanning electrochemical microscopy - a new technique for the characterization and modification of surfaces. *Accounts of Chemical Research,* 1990;23;357-363.

[20] Mansikkamaki K, Ahonen P, Fabricius G, Murtomaki L, Kontturi K. Inhibitive effect of benzotriazole on copper surfaces studied by SECM. *Journal of the Electrochemical Society,*2005;152:B12-B16.
[21] Mansikkamaki K, Johans C, Kontturi K. The Effect of Oxygen on the Inhibition of Copper Corrosion with benzotriazole. *Journal of the Electrochemical Society.* 2006;153:B22-B24.
[22] Mansikkamaki K, Haapanen U, Johans C, Kontturi K, Valden M. Adsorption of benzotriazole on the surface of copper alloys studied by SECM and XPS *Journal of the Electrochemical Society.* 2006;153:B311-B318.
[23] Izquierdo J, Santana JJ, González S, Souto RM. Uses of scanning electrochemical microscopy for the characterization of thin inhibitor films on reactive metals: The protection of copper surfaces by benzotriazole. *Electrochimica Acta.* 2010, submitted.
[24] Hubbard AT, Anson FC. The theory and practice of electrochemistry with thin layer cells. In: Bard AJ, ed. *Electroanalytical Chemistry*, vol. 4. New York: Marcel Dekker, New York; 1970:129-214.
[25] González-García Y, Burstein GT, González S, Souto RM. Imaging metastable pits on austenitic stainless steel *in situ* at the open-circuit corrosion potential. *Electrochemistry Communications.* 2004;6:637-642.
[26] Bastos AC, Simões AM, González S, González-García Y, Souto RM. Imaging concentration profiles of redox-active species in open-circuit corrosion processes with the scanning electrochemical microscope. *Electrochemistry Communications.* 2004;6:1212-1215.
[27] Gabrielli C, Ostermann E, Perrot H, Vivier V, Beitone L, Mace C. Concentration mapping around copper microelectrodes studied by scanning electrochemical microscopy. *Electrochemistry Communications.* 2005;7:962-968.
[28] Volker E, Inchauspe CG, Calvo EJ. Scanning electrochemical microscopy measurement of ferrous ion fluxes during localized corrosion of steel. *Electrochemistry Communications.* 2006;8:179-183.
[29] Simões AM, Bastos AC, Ferreira MG, González-García Y, González S, Souto RM. Use of SVET and SECM to study the galvanic corrosion of an iron - zinc cell. *Corrosion Science.* 2007:49;726-739.
[30] Yin Y, Niu L, Lu M, Guo W, Chen S. In situ characterization of localized corrosion of stainless steel by scanning electrochemical microscope. *Surface Science.* 2009;255:9193–9199.
[31] González-García Y, Souto RM, Daniele S. Microelectrochemical detection of zinc species in corrosion processes. Under preparation.
[32] Ciani I, Daniele S, Bragato C, Baldo MA. Stability of mercury-coated platinum microelectrodes upon touching a solid surface in scanning electrochemical microscopy (SECM) experiments. *Electrochemistry Communications.* 2003;5:354-358.
[33] Janotta M, Rudolph D, Kueng A, Kranz C, Voraberger HS, Waldhauser W, Mizaikoff B. Analysis of corrosion processes at the surface of diamond-like carbon protected zinc selenide waveguides. *Langmuir.* 2004;20:8634-8640.
[34] Burstein GT, Liu C, Souto RM, Vines SP. Origins of Pitting Corrosion. *Corrosion Engineering Science and Technology.* 2004;39:25-30.
[35] Still JW, Wipf DO. Breakdown of the iron passive layer by use of the scanning electrochemical microscope. *Journal of the Electrochemical Society.* 1997;144:2657-2665.
[36] Gabrielli C, Joiret S, Keddam M, Perrot H, Portail N, Rousseau P, Vivier V. A SECM assisted EQCM study of iron pitting. *Electrochimica Acta.* 2007;52:7706-7714.
[37] Gabrielli C, Joiret S, Keddam M, Portail N, Rousseau P, Vivier V. Single pit on iron generated by SECM. An electrochemical impedance spectroscopy investigation. *Electrochimica Acta.* 2008;53:7539-7548.
[38] Souto RM, Fernández-Mérida L, González S. SECM imaging of interfacial processes in defective organic coatings applied on metallic substrates using oxygen as redox mediator. *Electroanalysis.* 2009;21:2640-2646.
[39] Santana JJ, González-Guzmán J, Fernández-Mérida L, González S, Souto RM. Visualization of local degradation processes in coated metals by means of scanning electrochemical microscopy in the redox competition mode. *Electrochimica Acta.* 2010;55:4488-4494.
[40] Eckhard K, Chen XX, Turcu F, Schuhmann W. Redox competition mode of scanning electrochemical microscopy (RC-SECM) for visualisation of local catalytic activity. *Physical Chemistry Chemical Physics.* 2006;8:5359-5365.
[41] Karnicka K, Eckhard K, Guschin DA, Stoica L, Kulesza PJ, Schuhmann W. Visualisation of the local bio-electrocatalytic activity in biofuel cell cathodes by means of redox competition scanning electrochemical microscopy (RC-SECM). *Electrochemistry Communications.* 2007;9:1998-2002.
[42] Bastos AC, Simões AM, González S, González-García Y, Souto RM. Application of the scanning electrochemical microscope to the examination of organic coatings on metallic substrates. *Progress in Organic Coatings.* 2005;53:177-182.
[43] Horrocks BR, Mirkin MV, Pierce DT, Bard AJ, Nagy G, Toth K. Scanning electrochemical microscopy. 19. Ion-selective potentiometric microscopy. *Analytical Chemistry.* 1993;65:1213-1224.
[44] Wei C, Bard AJ, Nagy G, Toth K. Scanning electrochemical microscopy. 28. Ion-selective neutral carrier-based microelectrode potentiometry. *Analytical Chemistry.* 1995; 67:1346-1356.
[45] Park JO, Paik CH, Alkire RC. Scanning microsensors for measurement of local pH distributions at the microscale. *Journal of the Electrochemical Society.* 1996;143:L174-L176.
[46] Hayase M, Hatsuzawa T, Fukuizumi A. Electric field analysis in a dilute solution for the vibrating electrode technique. *Journal of Electroanalytical Chemistry.* 2002;537:173-181.
[47] Lamaka SV, Karavai OV, Bastos AA, Zheludkevich ML, Ferreira MGS, Monitoring local spatial distribution of $Mg^{2+}$, pH and ionic currents. *Electrochemistry Communications.* 2008;10:259-262.
[48] Ballesteros Katemann B, Schulte A, Schuhmann W. Constant-distance mode scanning electrochemical microscopy (SECM) - Part I: Adaptation of a non-optical shear-force-based positioning mode for SECM tips. *Chemistry-A European Journal.* 2003;9:2025-2033.
[49] Etienne M, Schulte A, Mann S, Jordan G, Dietzel ID, Schuhmann W. Constant-distance mode scanning potentiometry.1. Visualization of calcium carbonate dissolution in aqueous solution. *Analytical Chemistry.* 2004;76:3682-3688.